3. OBSERVED RESPONSE OF THE BRIDGE AND THE SURROUNDING SOIL

The 1995 Hyogoken-nambu Earthquake

Figure 7 presents time histories of acceleration response of the Higashi-Kobe Bridge and the surrounding soil during the 1995 Hyogoken-nambu (Kobe) Earthquake. The records at the top (T1, c.f. Figure 2) are overscaled, and are not shown in the figure. The transverse component at point T2 is also slightly overscaled. The maximum accelerations, velocities and displacements at each observation point are presented in Table 2. As it can be seen from the time history of the downhole accelerometer G2 (GL-34.0 m. c.f. Figure 2), the near-fault ground motions include large pulses with long period, which are potentially damaging to multistory buildings and bridges. Despite this harsh test, the Higashi-Kobe Bridge performed outstandingly during the Kobe Earthquake. The only sustained damage was to a wind shoe at one of the secondary piers on the west side in Uozaki-hamamachi.

The time history of acceleration at the main girder level (T3, Figure 7(c)) shows multiple pulses followed by decaying vibrations towards the coda of the record. If a cable has been relaxed in a certain moment and its tensile resistance has been engaged in the next moment, the sudden restriction on the motion of the main girder will load the structure with an impulse. The occasional pounding with the adjacent part of the highway should be expected to cause a similar effect.

Comparing the time histories recorded by the downhole soil accelerometer G1, (GL -34.0 m) and the surface accelerometer G2 (GL-1.5m, c.f. Figure 2), it can be seen that the acceleration at the surface is smaller than the one at 34 m depth and exhibits longer period motion. These observations suggest that the surface soil layers, which consist of loose saturated sands, have been liquefied during the earthquake. This hypothesis is confirmed numerically in the following discussion. Evidently, within the duration of the event, the soil properties underwent significant changes. Nonstationary response analysis was performed to investigate the effects of these changes for the purposes of numerical simulation of the soil-structure system behavior. Figure 8 presents evolutionary response spectra of the longitudinal motion at depth 34 m and at the ground surface. It can be seen that the peak values diminish at frequencies above 5 Hz and outside of the time interval 10-20 seconds.

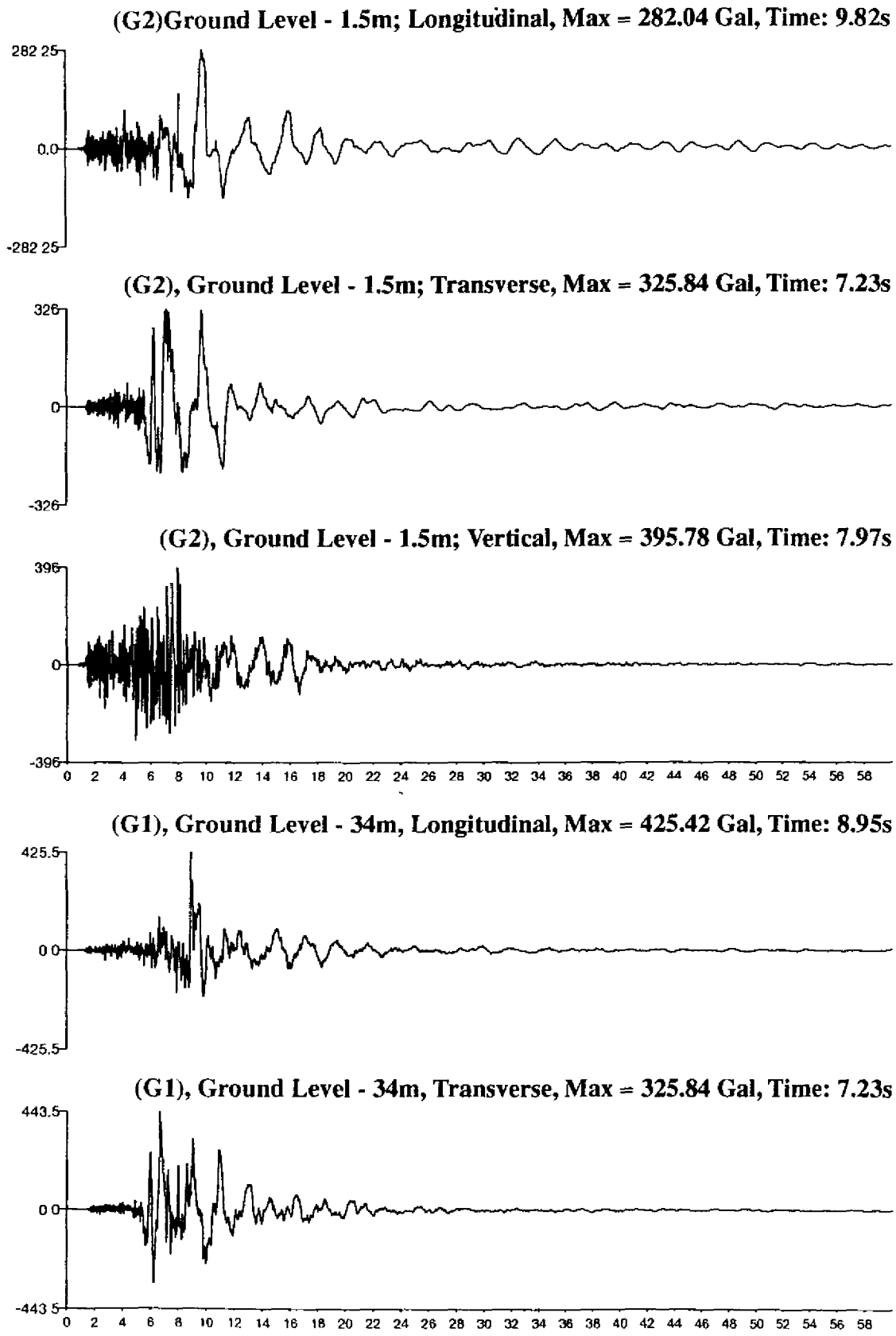

Figure 7 a) Downhole and surface soil

TABLE 2. MAXIMUM RECORDED RESPONSE TO THE 1995 HYOGOKEN-NAMBU EARTHQUAKE

Name and position	Orientation	Acceleration [cm/s^2]	Velocity [cm/s]	Displacement [cm]
G1 (GL -34m)	Longitudinal	425.4	71.2	27.8
	Transverse	443.4	76.0	34 3
G2 (GL -1.5m)	Longitudinal	282 0	84.5	51.2
	Transverse	325 8	90.7	49.5
	Vertical	395.8	35.0	14.9
K1 (Bottom of foundation at P24)	Longitudinal	333.9	77.5	34.0
	Transverse	354.9	79.1	39.4
	Vertical	389.3	34.1	12.6
T2 (Middle of tower at P24)	Longitudinal	385.7	29.1	18.7
	Transverse	1000*	225.1**	117.6**
T3 (Tower at P24, level of main girder)	Longitudinal	596.3	90.7	33 9
	Transverse	806.5	105.7	51 3
	Vertical	806.7	71.1	37.8

Notes: (*) - Overscaled gauge, (**) - The value is calculated from an overscaled record

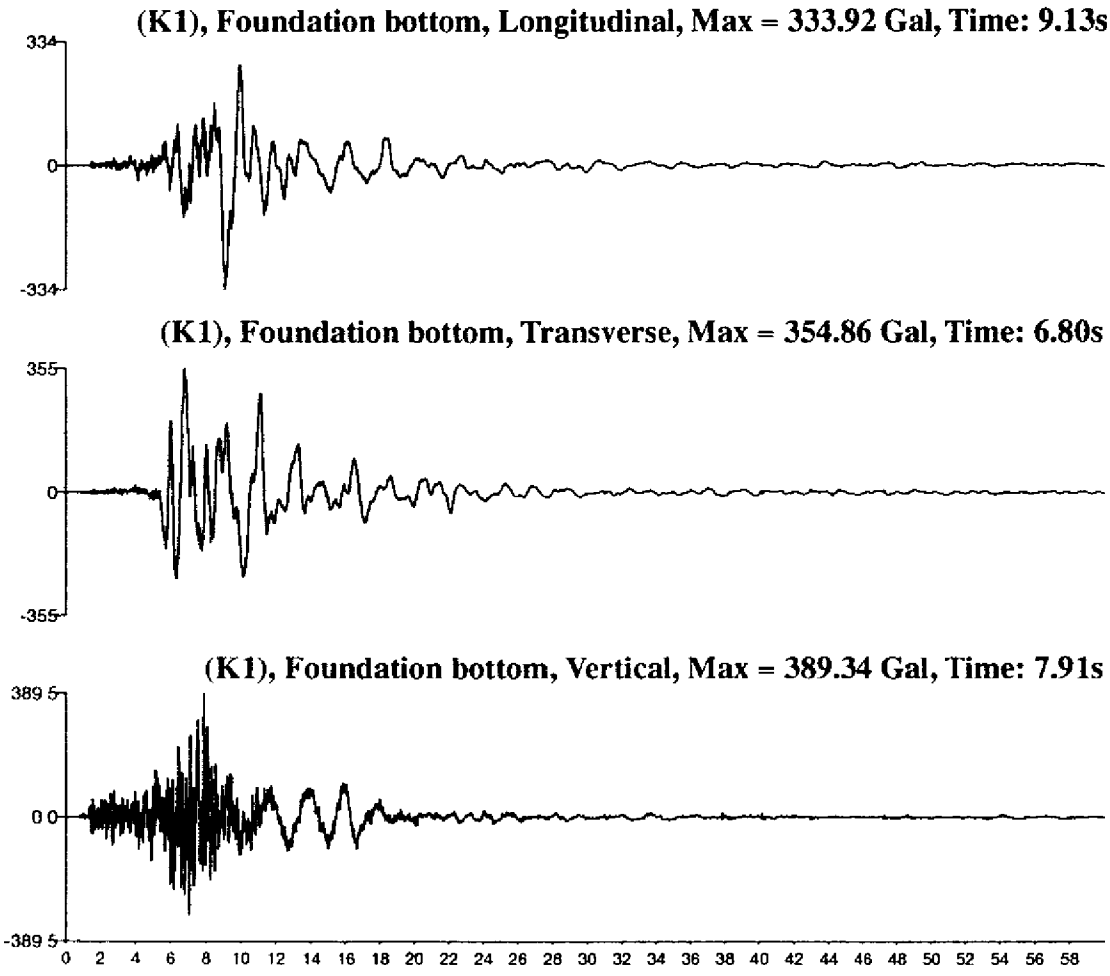

Figure 7. b) Bottom of caisson foundation at P25

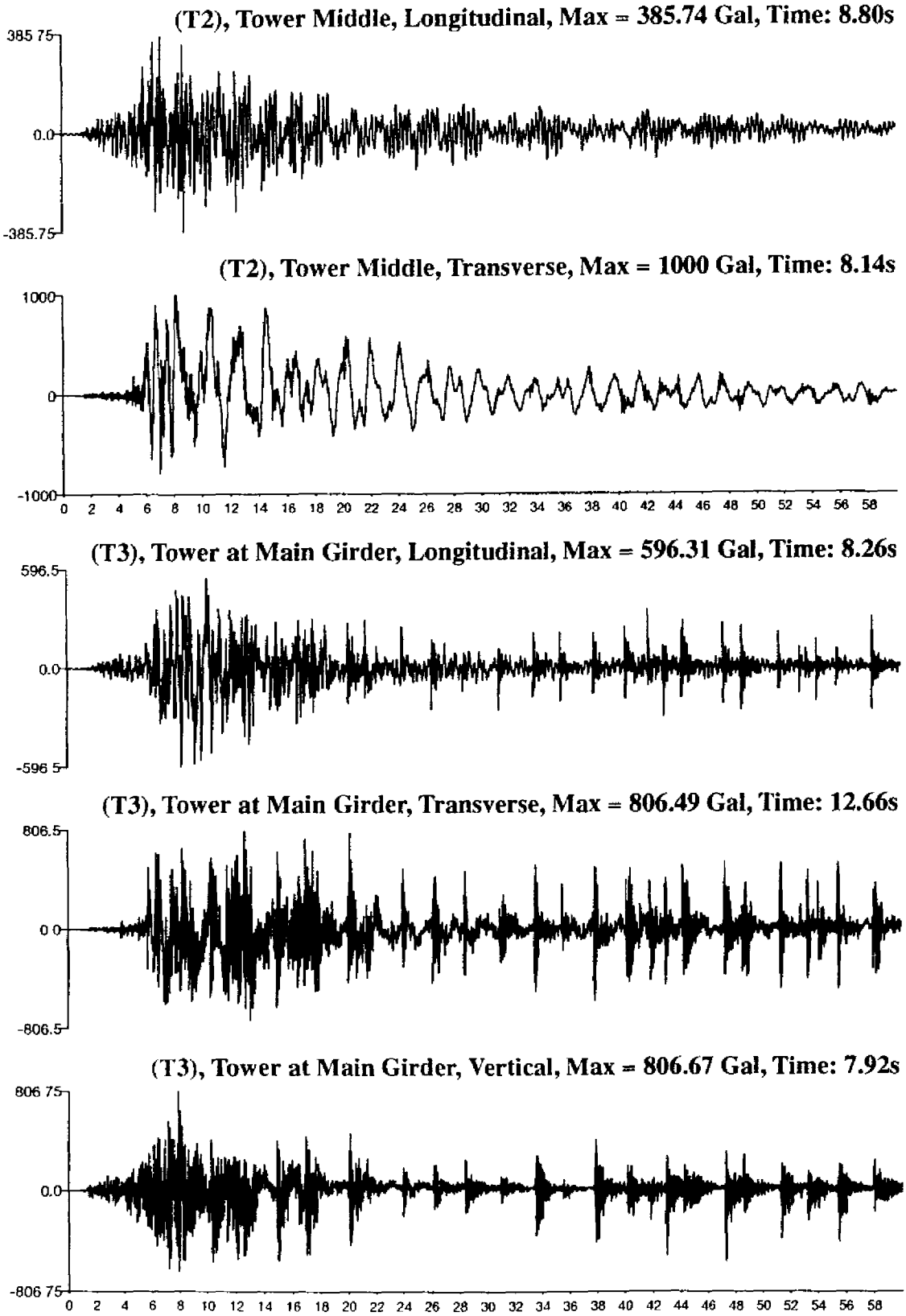

Figure 7. c) Tower response at middle and main girder levels

Figure 7. Time histories of acceleration of the Hyogoken-nambu Earthquake

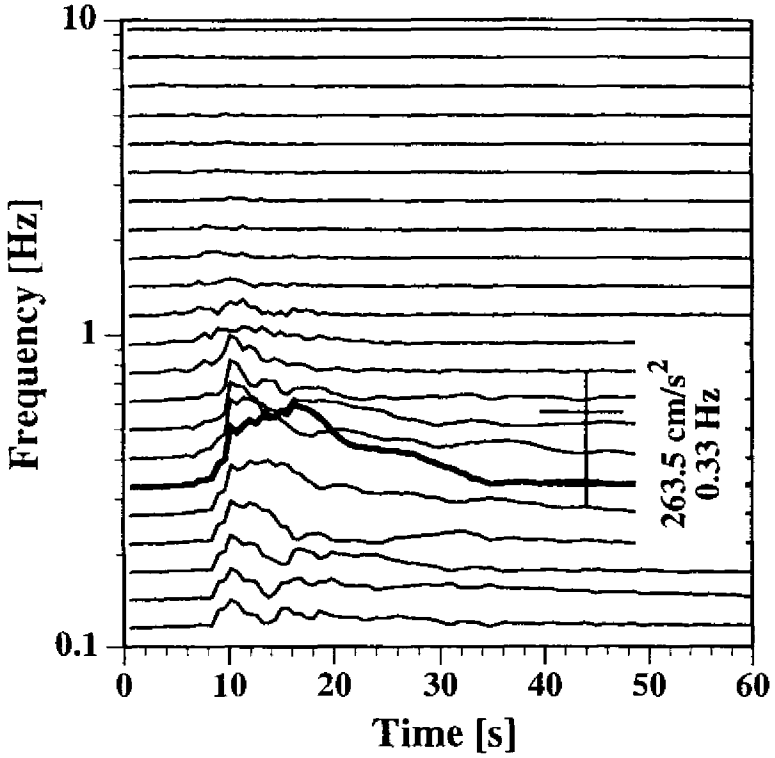

a) Ground level -1.5 m, longitudinal component

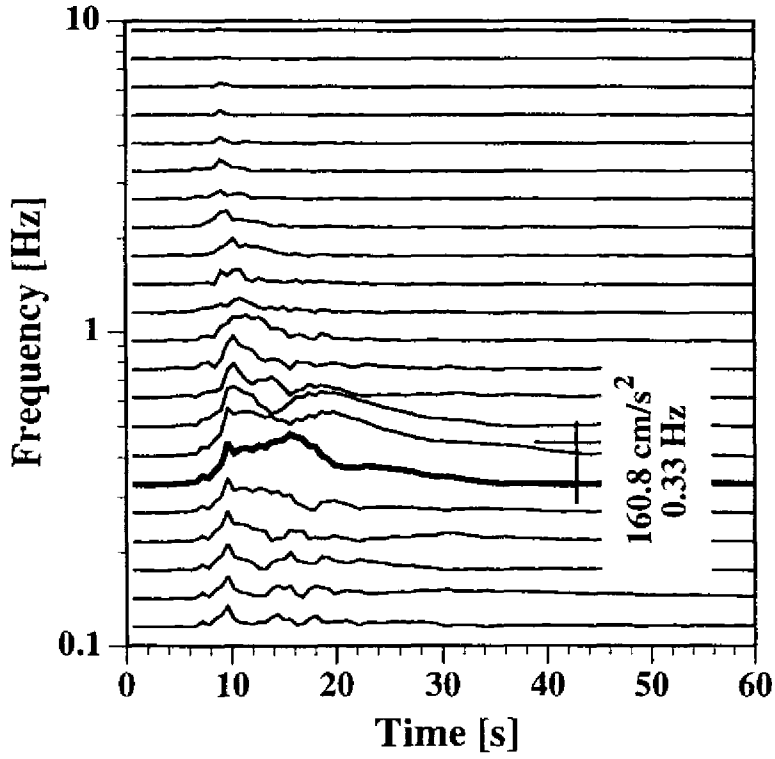

b) Ground level -34.0 m, longitudinal component

Figure 8. Evolutionary response spectra of ground motion

Figure 9 offers results of stationary analysis of the same records. It compares Fourier spectrum ratios between the downhole and the surface acceleration for three time intervals. In the initial 5 seconds, amplification is observed. During the strong motion, the amplitude ratios are much lower, which can be explained with the occurrence of liquefaction. At the coda of the record, complete liquefaction of the surface layers greatly suppresses the energy transfer. Similar results are obtained by analysis in the transverse direction.

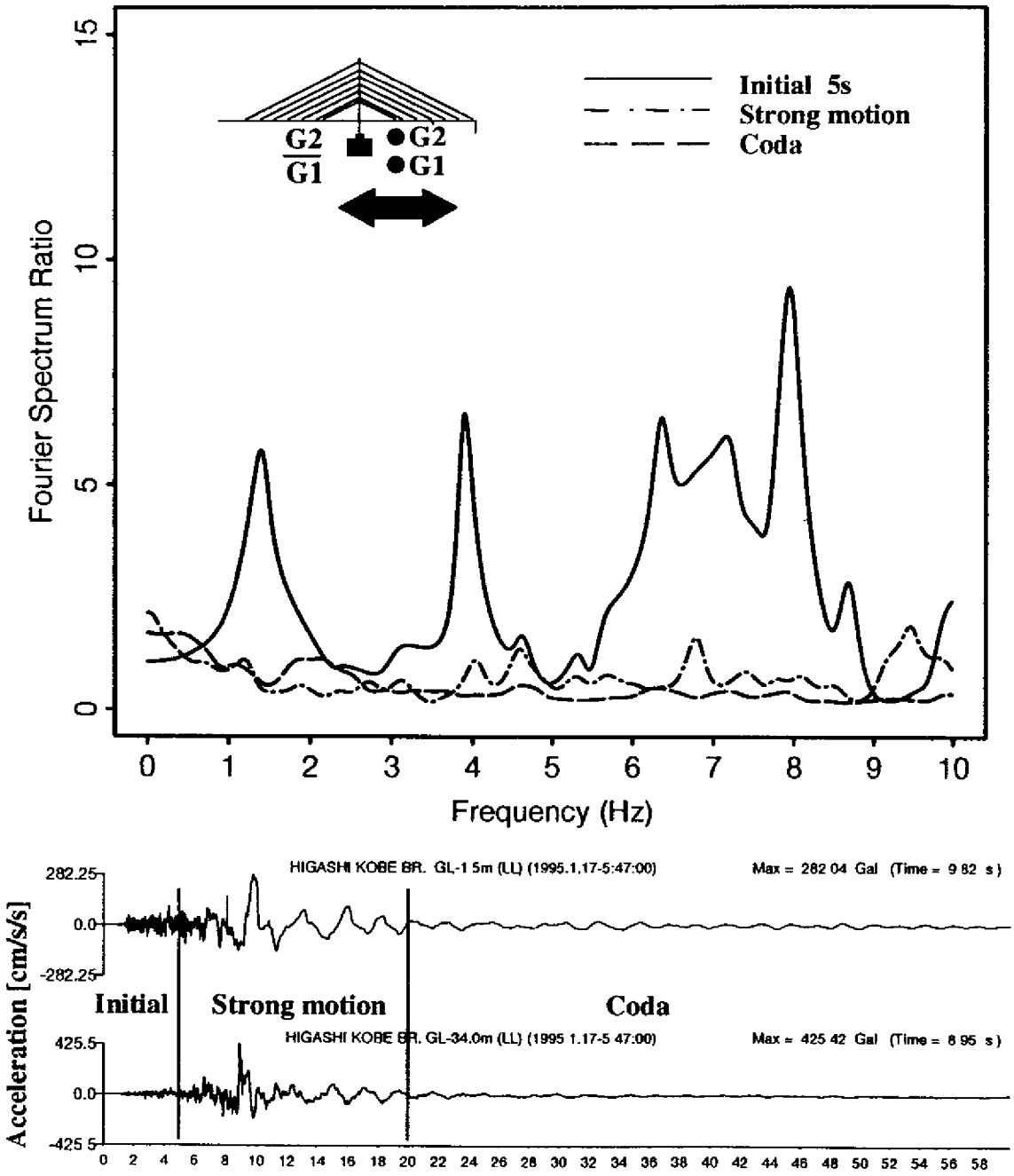

Figure 9. Fourier spectrum ratios between surface and downhole ground acceleration records (longitudinal direction)

Comparison with a small earthquake

To assess the effect of the soil-structure interaction effects in a large earthquake a comparison was made with the behavior of the system in a small event, which occurred on January 25, 1996 and had a peak ground acceleration of 42.5 cm/s^2. Its characteristics are summarized in Table 3. Figure 10 presents Fourier spectrum ratios between the free field at depth 34 m and the mid-height of the bridge tower, evaluated from the records of the Hyokogen-nanbu Earthquake and from the small event. Since the tower is tall, slender and flexible, its elastic response dominates the total response and sway and rocking modes of motion have a secondary influence. In this way, the soil stiffness degradation does not lead to substantial shift of the predominant frequency of the system, as is often observed for shorter, squatter and rigid structures.[3,4),8)] The alteration of the soil behavior affects mainly the amplitude of the response.

TABLE 3. MAXIMUM RECORDED RESPONSE TO A SMALL EARTHQUAKE OF JANUARY 1996

Name and position	Orientation	Acceleration [cm/s^2]	Velocity [cm/s]	Displacement [cm]
G1 (GL -34m)	Longitudinal	25.0	1.5	0.13
	Transverse	23.0	1.5	0.07
G2 (GL -1.5m)	Longitudinal	42.0	2.6	0.26
	Transverse	31.0	1.6	0.13
	Vertical	24.0	1.0	0.07
K1 (Bottom of foundation at P24)	Longitudinal	15.0	1.5	0.15
	Transverse	13.0	1.0	0.08
	Vertical	13.0	0.9	0.04
T2 (Middle of tower at P24)	Longitudinal	31.0	1.5	0.09
	Transverse	11.0	1.6	0.14
T3 (Tower at P24, level of main girder)	Longitudinal	66.0	3.8	0.32
	Transverse	65.0	1.9	0.13
	Vertical	19.0	0.9	0.05

4. NUMERICAL SIMULATION OF DYNAMIC RESPONSE

Modeling considerations

Considering the necessity to take into account soil-structure interaction, analysis was performed with the program SASSI employing the flexible volume substructuring approach[5)]. Taking advantage of the symmetry, a quarter model of the bridge was used. Based on the observations in the previous section, it was determined that an adequate frequency range for analysis would be up to 5 Hz. As the maximum frequency of analysis also determines the maximum size of the finite elements, this choice also led to a reasonably efficient model. A conceptual scheme of the discretization of the foundation and the near-field soil with solid prismatic elements is shown in Figure 11. Figure 12 shows a cross-section of the same region and indicates the soil types. The characteristics of each soil type can be found in Table 4

for different analysis stages. Determination of parameters for the Hyogoken-nambu Earthquake is discussed in the following sections.

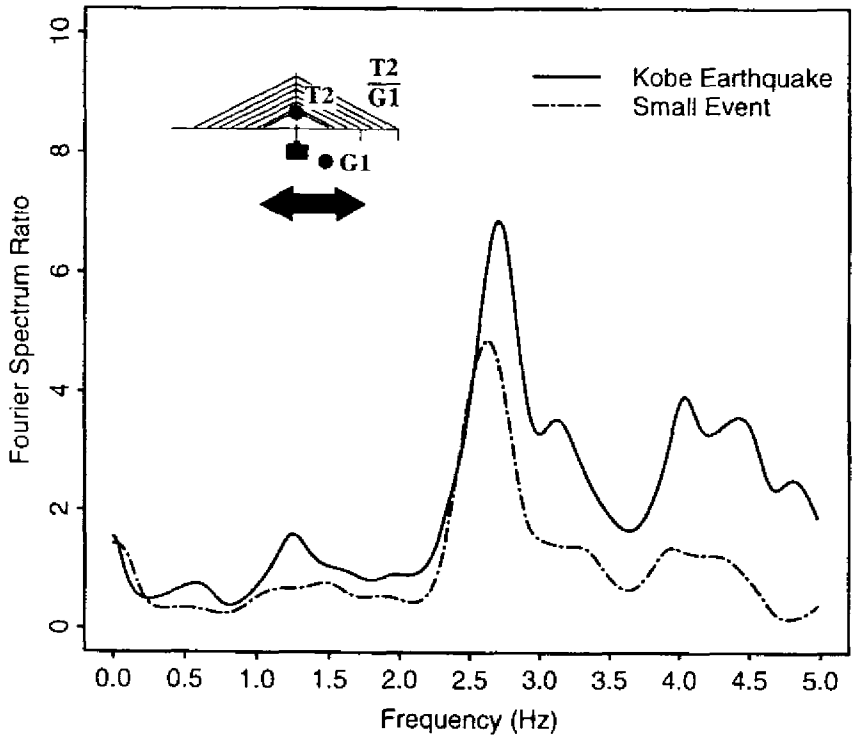

Figure 10. Comparison of Fourier spectrum rations evaluated from large and small earthquakes (longitudinal direction)

TABLE 4. SOIL PROPERTIES USED FOR DYNAMIC ANALYSIS IN LONGITUDINAL DIRECTION

Soil type	Small earthquake				The Hyogoken-nambu Earthquake			
	Shear wave velocity [m/s] V_S	Poisson ratio ν	Unit weight kN/m^3 γ	Damping ratio [%] D	Shear wave velocity [m/s] V_S	Poisson ratio ν	Unit weight kN/m^3 γ	Damping ratio [%] D
1	151	0.48	18.0	3.3	20	0 48	18.0	12.0
2	144	0.48	18 0	5.6	30	0.48	18.0	12.0
3	271	0.44	18.0	3.6	40	0.44	18.0	12 0
4	269	0.44	18.0	4.0	40	0.44	18.0	12.0
5	107	0.49	16.0	5.3	70	0.49	16.0	10.0
5a	107	0.49	15.0	5.3	70	0.49	15.0	8.0
6	116	0.49	16.0	3.8	50	0.49	16.0	10.0
6a	116	0.49	15.0	3.8	50	0.49	15.0	10.0
7	302	0.48	19.0	3.2	234	0.48	19.0	5.0
8	363	0.47	19.5	2.8	297	0.47	19.5	3.3
9	238	0.49	19 5	0.4	196	0.49	19.5	3.0
10	331	0.48	19.5	3.0	317	0.48	19.5	7.1
11	207	0.49	19.5	0.7	198	0.49	19.5	7.1
12	410	0.49	19.5	0.2	380	0.49	19.5	7.1

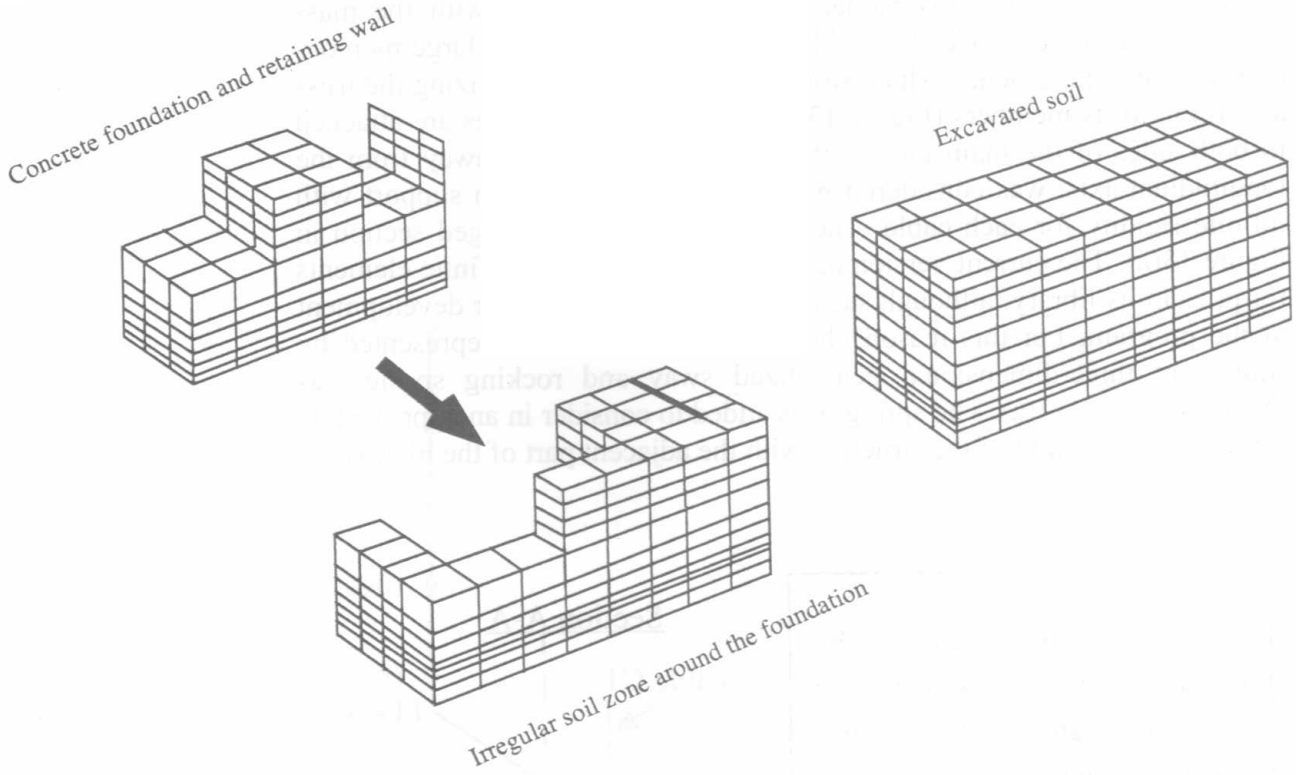

Figure 11. Discretization of the foundation and near-field soil at P24 with SASSI

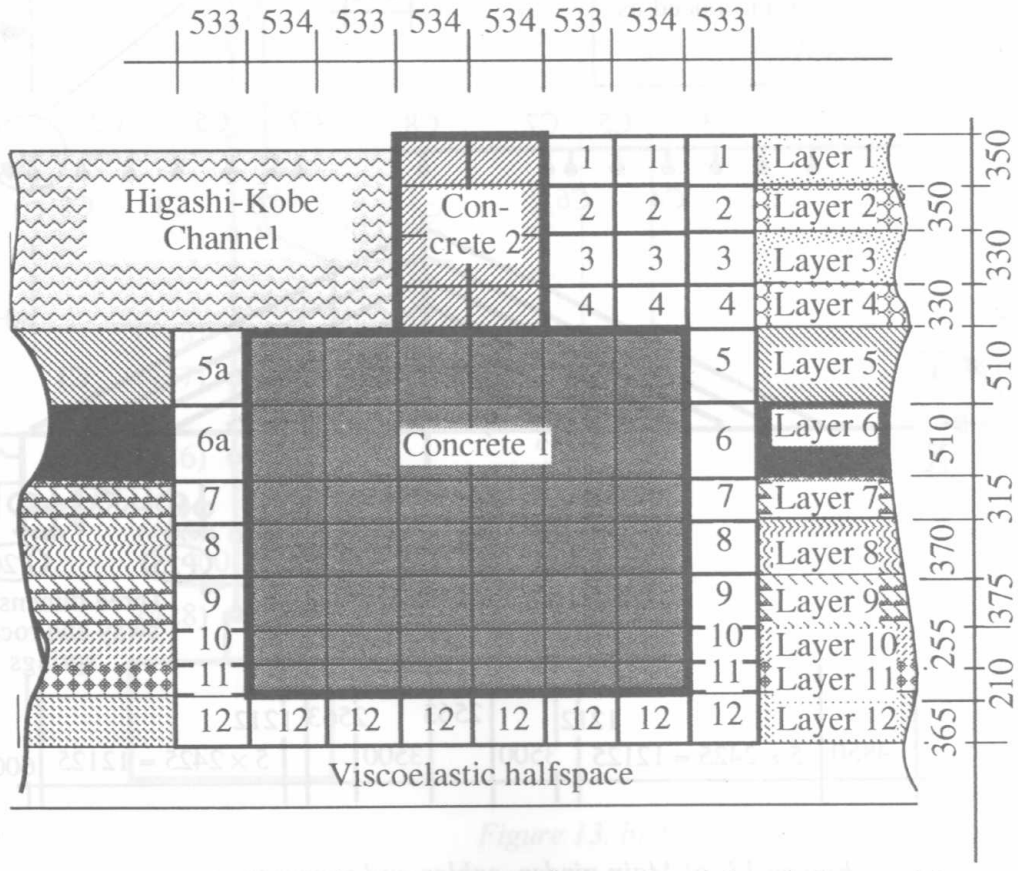

Figure 12. Vertical cross-section of the soil and foundation model

The superstructure was modeled with beam elements with the mass concentrated in their nodes to avoid lengthy calculations and large memory and storage requirements, which would be imposed by discretizing the truss according to its members (Figure 13). The fact, that the cables are attached to both sides of the main girder, at a distance of 8 meters away from the longitudinal axis, was considered by attaching a lateral beam support with infinite rigidity for each cable. They are shown in the enlarged section in Figure 13(a). The current version of SASSI does not include finite elements for piles in its library, although such are planned in the further development of the program. For this reason, the pile foundations were represented by equivalent three-dimensional generalized sway and rocking springs, as shown in Figure 13(a). The spring S_1 is added to consider in an approximate manner the pounding of the structure with the adjacent part of the highway.

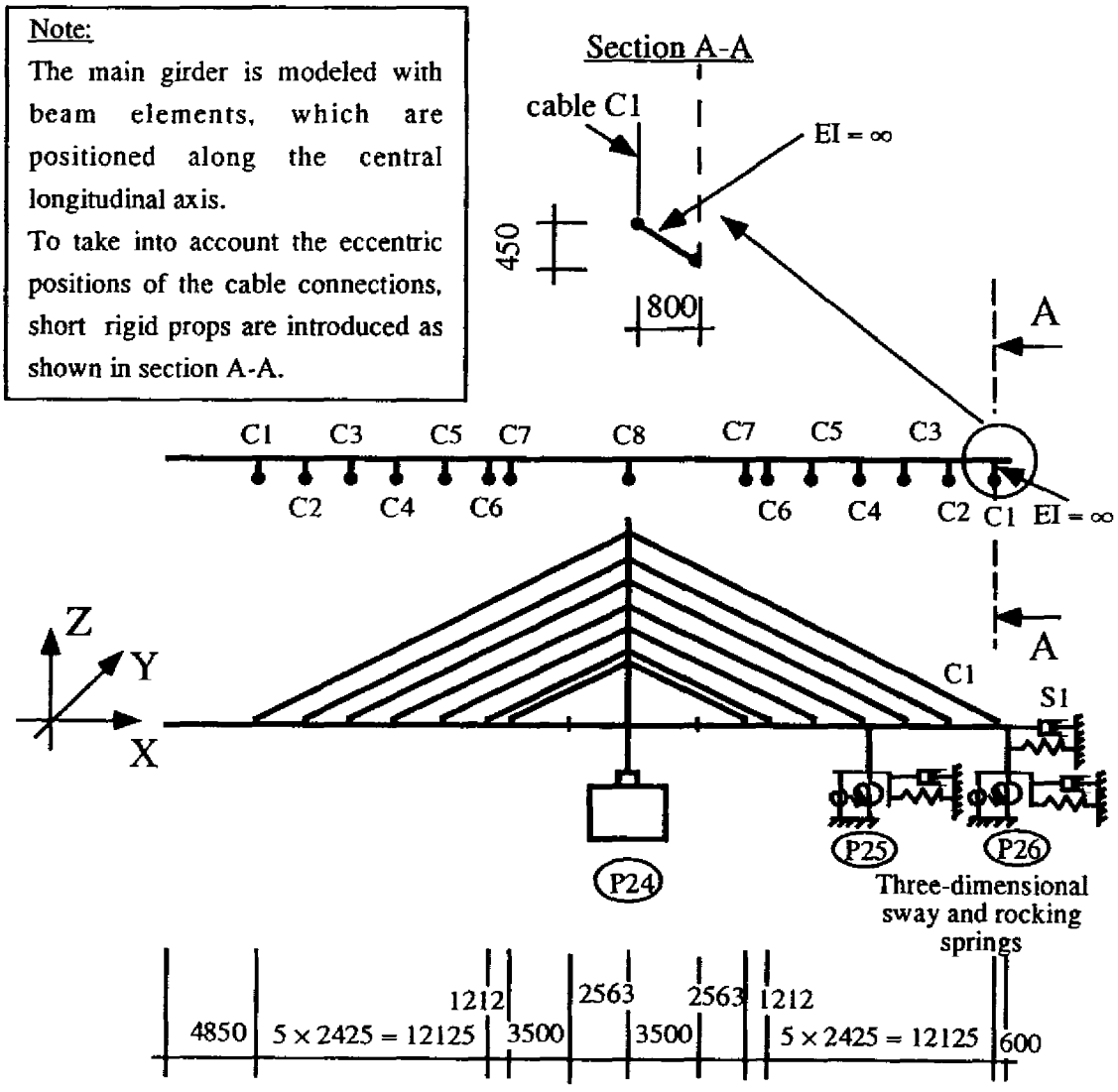

Figure 13. a) Main girder, cables and supports

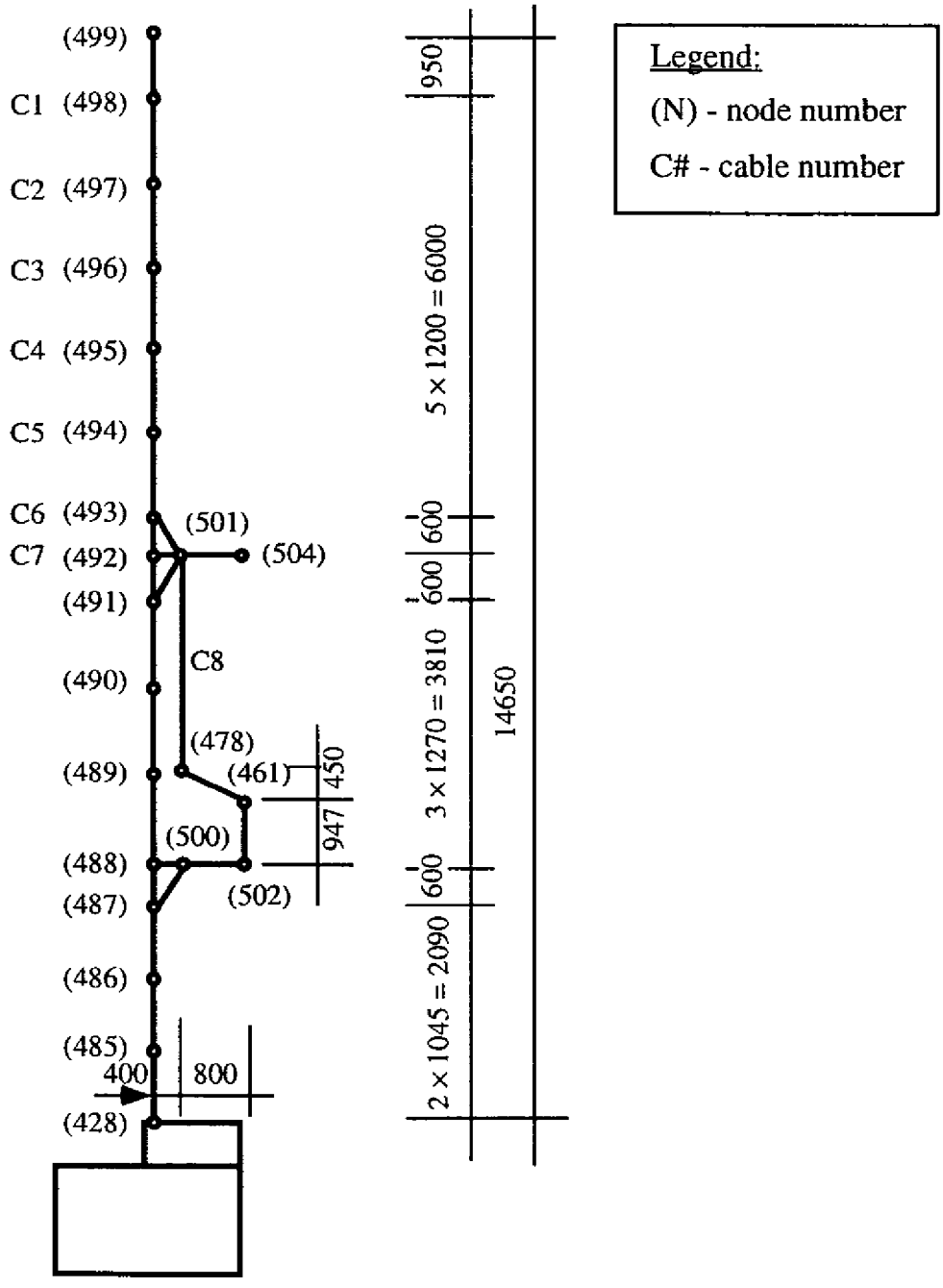

Figure 13 b) Tower at P24

Figure 13. Finite element discretization of the superstructure

An additional modeling consideration was the cable action, since the only appropriate elements in the SASSI library are of beam type and have compression stiffness. The effect of the error of using beam elements for modeling of the cables was investigated with the program MSC/NASTRAN[9], using as dynamic excitation the small earthquake of January 1996 (Table 3). The cables were modeled once with a combination of gap and spring elements and nonlinear dynamic analysis was performed, considering the initial tensile stress in the elements due to gravity. The solution was compared to a linear solution with beam elements. It was found, that with the given geometrical disposition of the cables, the tension forces in them from gravity are large enough to create effective compression resistance almost equal to their tensile stiffness. In this way it was judged, that linear analysis with beam elements would be a reasonable approximation and it is justifiable to use SASSI. Obviously, the error would depend on the magnitude of the displacements and would be larger for a stronger earthquake. For the MSC/NASTRAN analysis only, the soil support at the P24 foundation was modeled with equivalent three-dimensional generalized springs, evaluated on the basis of the Continuum Formulation Method.[3,4),10)] As the main purpose of these calculations was to validate the superstructure model, the soil spring action is not discussed here.

Small-strain linear dynamic response

At the initial stage of the analysis, the behavior of the soil-structure system in the small-strain linear range was examined by simulating its response to the small earthquake described by Table 3. Equivalent stiffness and damping characteristics of the soil were determined using the program SHAKE on the basis of the one-dimensional wave propagation theory. The results of this analysis validated the use of initial soil properties as well as the model of the superstructure. In conjunction with nonlinear dynamic analysis performed with MSC/NASTRAN, it helped determine the modeling of the cable action as discussed in the previous section. Figure 14(a) compares the Fourier spectrum ratio of the recorded surface and downhole soil records with the calculated by SASSI. The good agreement signifies that the soil model is adequate. Figure 14(b) shows the recorded and calculated Fourier Spectrum ratios between the free field surface and the mid-height of the tower. The excellent coincidence validates the superstructure model. The time histories of recorded and calculated response at mid-height of the bridge tower are visualized in Figure 14(c) to confirm the adequacy of the frequency domain results.

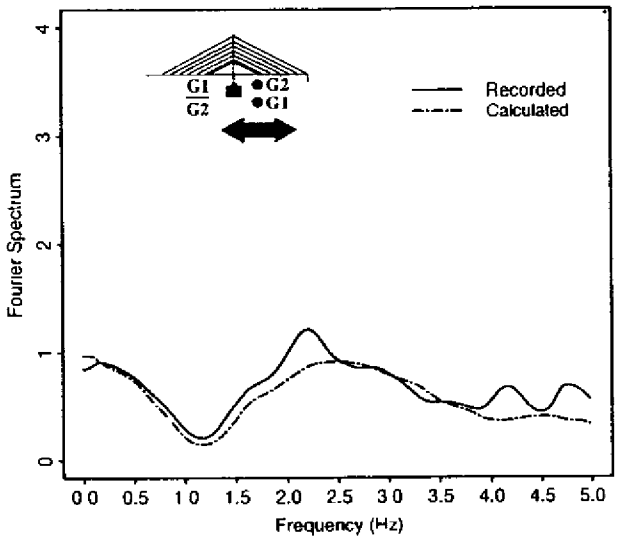

a) Amplitude ratios of deep to surface ground motion

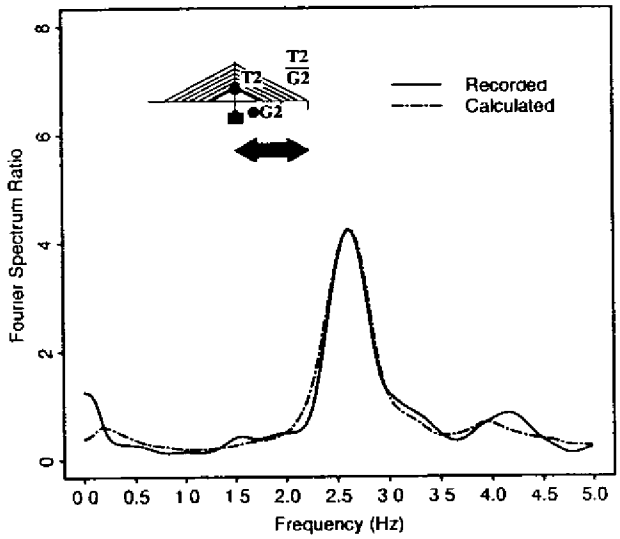

b) Amplitude ratios between the ground surface motion and response at mid-height of the bridge tower (longitudinal component)

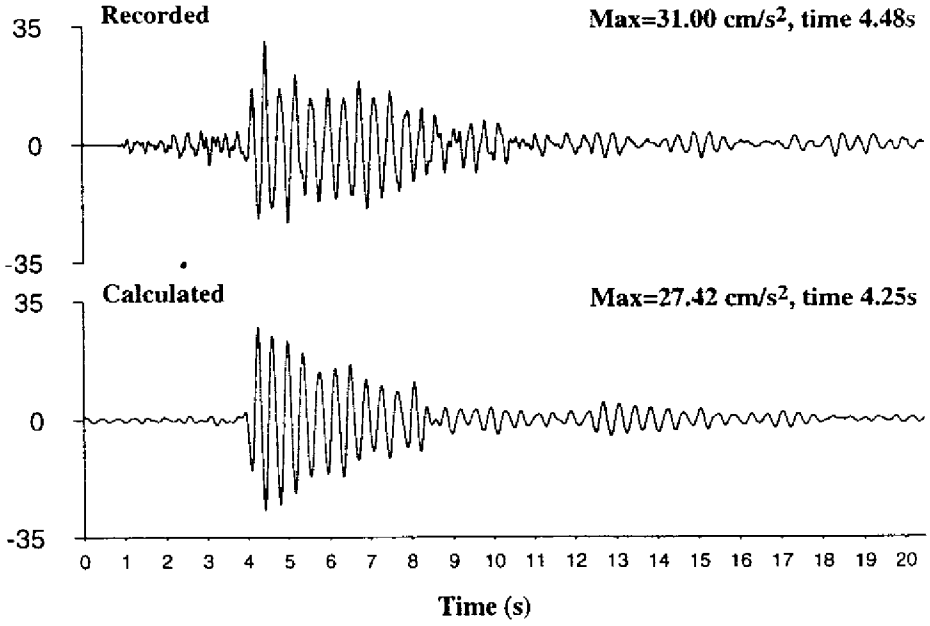

c) Time histories of recorded and simulated acceleration response at mid-height of the bridge tower (longitudinal component)

Figure 14. Simulation of the response to a small earthquake

Dynamic response in the large strain range

Analysis of the soil response in the main shock of the Hyogoken-nambu Earthquake with SHAKE produced inadequate results and an alternative method of determination of equivalent soil properties was necessary. The nonlinear behavior of the soil was investigated with a one-dimensional

effective stress analysis program[11]. In this simulation, the Ramberg-Osgood model[12] of stress-strain soil dependence is combined with a pore pressure buildup model based on shear work concept[13,14] to iteratively obtain soil characteristics and response in the time domain.

The input motion was specified by the acceleration record at depth 34m. Figure 15 shows a very good agreement between recorded and simulated soil response at the ground surface. The occurrence of liquefaction has been captured adequately by the model. Figure 16 shows a comparison between the maximum values of the excess pore-water pressure and initial effective stress. It is evident, that the soil was completely liquefied down to a depth of approximately 6m, which confirms the hypothesis formulated in the previous section. To a depth of 10 m the ratio of excess pore water pressure to initial effective vertical stress is about 86%, indicating that the soil in that region came to a state close to liquefaction. The time history of the ratio of the excess pore water pressure to the initial effective stress in the surface layer is plotted in Figure 17. The liquefaction of the surface layer can clearly be observed in the stress-strain curve plotted in Figure 18, which becomes increasingly distorted as the pore water pressure builds up.

Based on the above analysis, equivalent linear properties of the soil layers were determined. As the primary objective was to simulate the response of the structure to the strong motion part of the earthquake, values obtained by averaging the calculated soil stiffness in the period 8-10 s (c.f. Figure 7) were used. They are listed in Table 4. The time history of deep ground acceleration was used for seismic input as deconvolution of the surface record would be inaccurate under the conditions of liquefaction.

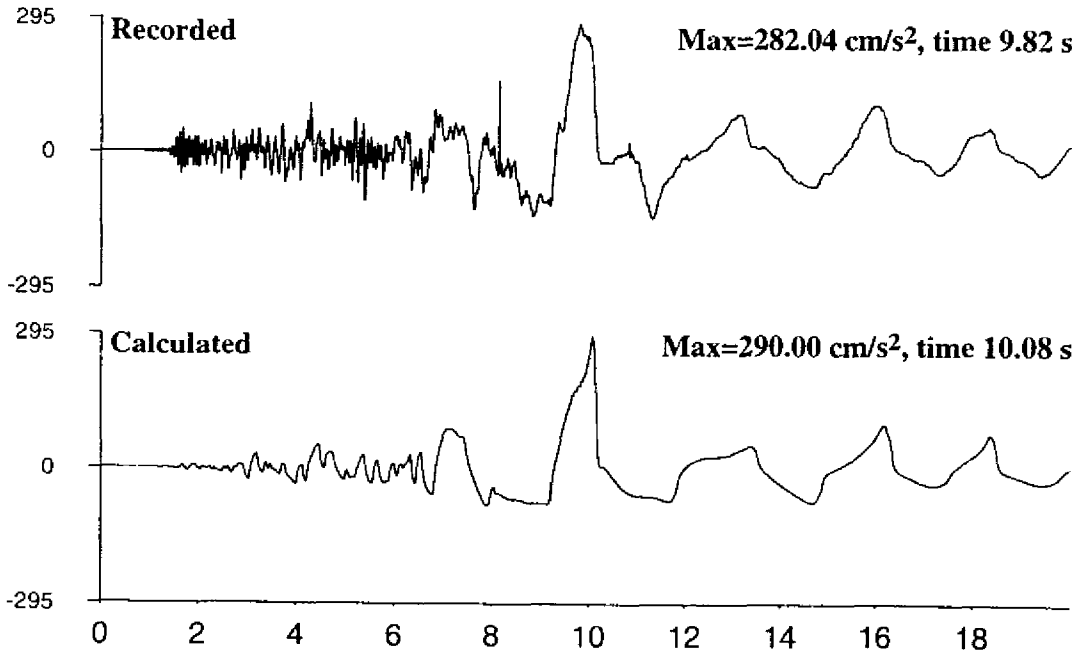

Figure 15. Time history of recorded and simulated acceleration response at the ground surface (longitudinal component)

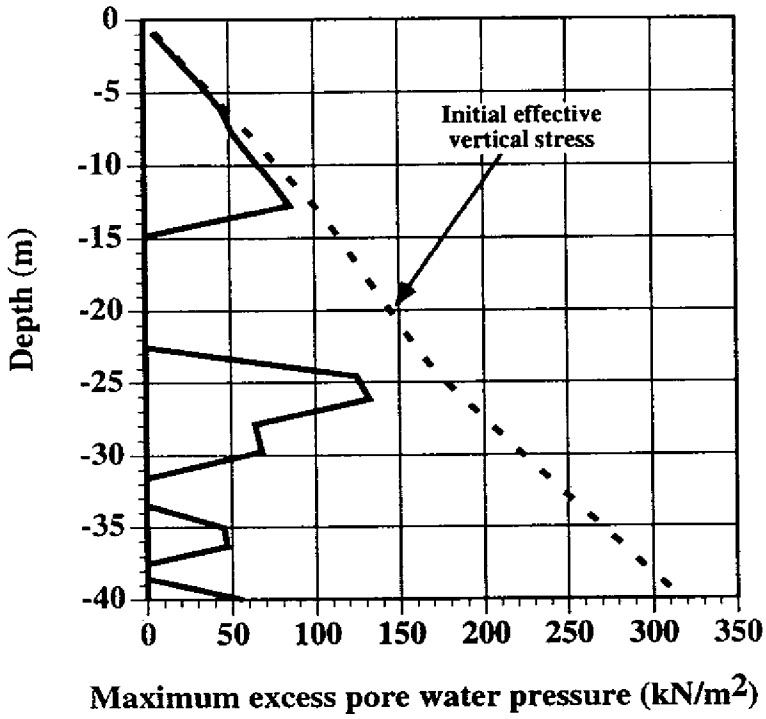

Figure 16. Distribution of maxumim excess pore water pressure with depth by the effective stress response analysis

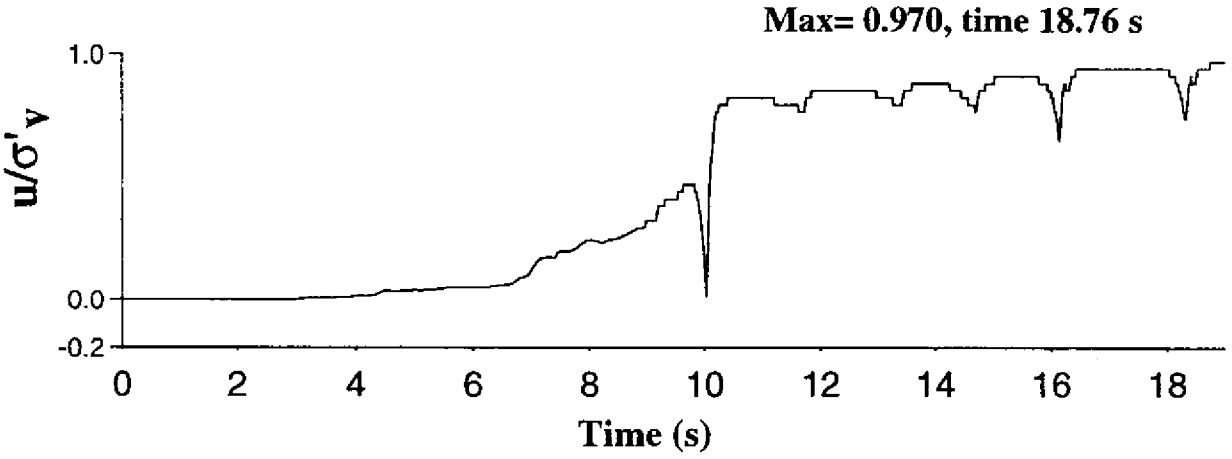

Figure 17. Time history of the ratio of the excess pore-water pressure to the initial effective stress by the effective stress analysis

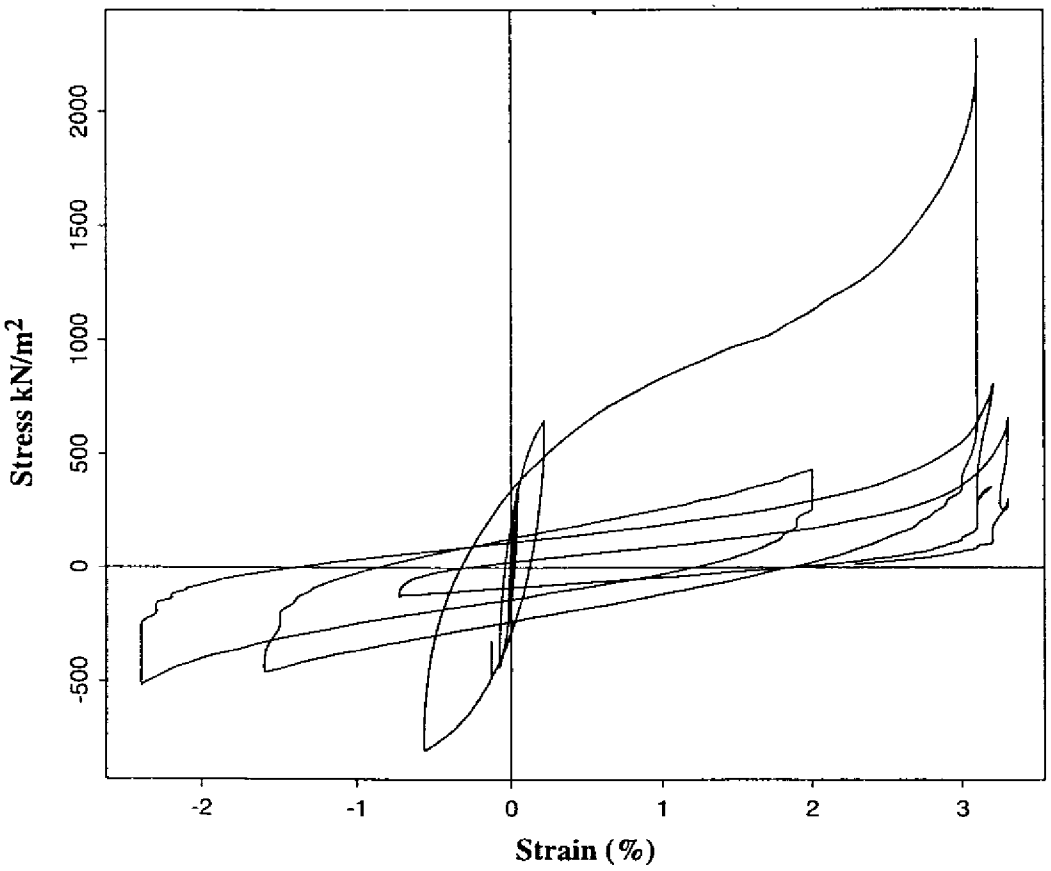

Figure 18. Stress-strain curve at the soil surface evaluated by effective stress analysis

Figure 19(a) compares the recorded and calculated Fourier Spectrum ratios between the deep ground motion and the response of the bridge tower at P24 at mid-height. The agreement is reasonably good, albeit worse than in the case of the small-strain response. It is evident that the equivalent linear soil parameters are not capable of producing a perfect simulation of the complicated nonlinear behavior, but offer a reasonable accuracy for practical purposes. The difference between recorded and calculated response in the range 4-5 Hz can be explained with the fact, that the equivalent averaged soil properties can not take into consideration the temporary recovery of soil stiffness during dynamic loading cycles and thus some of the higher frequency contents can not be simulated adequately. In addition, it should be noted, that the precision of the calculations with the given finite element mesh decreases with increasing of the frequency and diminishing of the shear wave velocity of the materials. Further vizualization is offered by comparing the time history of recorded and calculated acceleration at mid-height of the bridge tower (Figure 19(b)). The simulation follows the recorded response in general, but, as explained above, some high frequency components are filtered out. Additional reason for this discrepancy is the fact that the analysis is performed only up to a frequency of 5 Hz.

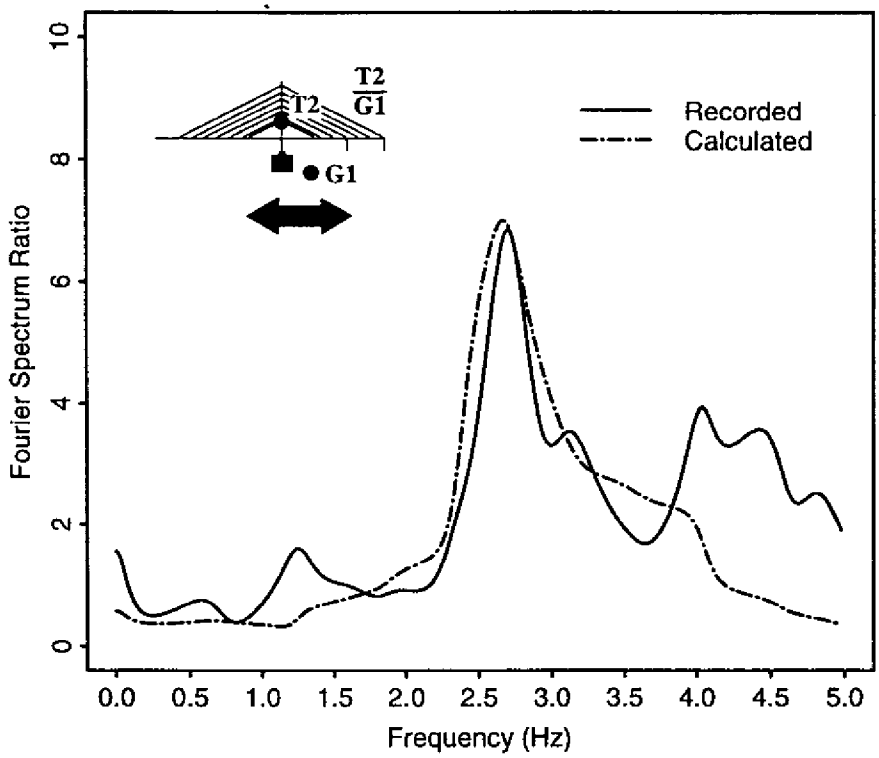

a) Amplitude ratios between the deep surface motion and response at mid-height of the bridge tower (longitudinal component)

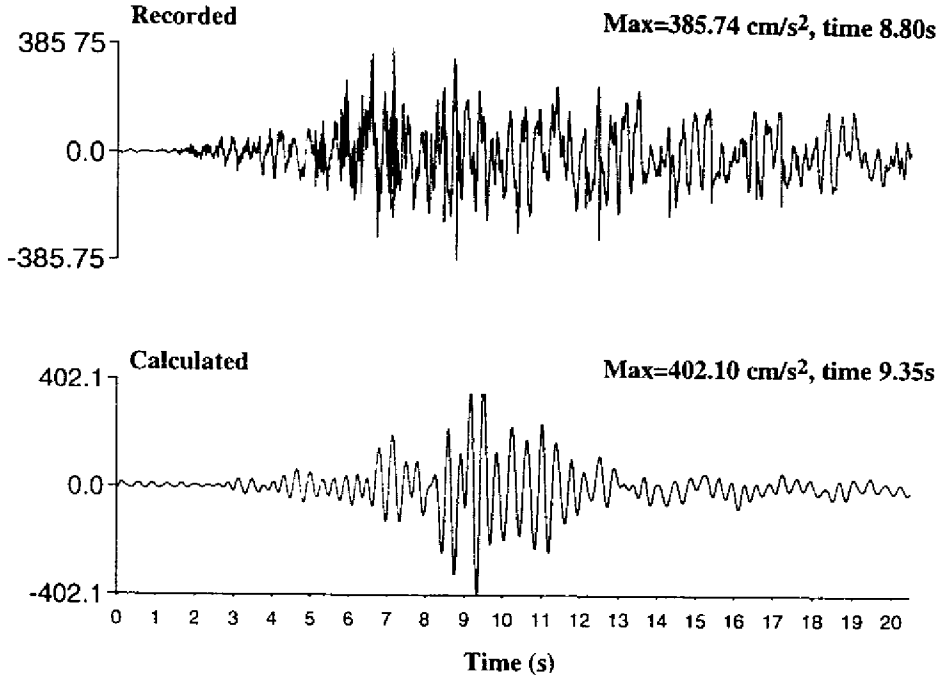

b) Time histories of recorded and simulated acceleration response at mid-height of the bridge tower (longitudinal component)

Figure 19 Simulation of the response to the 1995 Hyogoken-nambu Earthquake

5. CONCLUSIONS

The response of the Higashi-Kobe Bridge during the Hyogoken-nambu (Kobe) Earthquake of January 17, 1995, was analyzed with a finite element model employing flexible volume substructuring approach. The applied methodology was to simulate the complicated nonlinear soil and structural behavior separately and as rigorously as possible, in order to determine equivalent linear parameters for soil-structure interaction analysis with the program SASSI.

Both nonstationary and stationary analysis of the observed accelerograms were applied to identify the key phenomena affecting the performance of the bridge and the surrounding soil.

Soil and superstructure models were created and initially validated by accurately simulating the response to a small earthquake. Nonlinear dynamic analysis was performed with MSC/NASTRAN to investigate the error of modeling cables with beam elements in SASSI.

It was found that the response of the soil-structure system to the 1995 Hyogoken-nambu Earthquake had been strongly influenced by pore water pressure buildup in the saturated surface soil layers. Nonlinear effective stress analysis combining the Ramberg-Osgood stress-strain relation with a pore pressure model was performed to simulate the behavior of the free-field soil. Excellent agreement was achieved.

Equivalent soil parameters were evaluated on the basis of the liquefaction analysis and were used to perform soil-structure interaction analysis with SASSI. A reasonably good agreement was achieved. Even though the equivalent linear soil parameters are not capable of producing a perfect simulation of the complicated nonlinear behavior, the results offer a reasonable accuracy for practical purposes.

This case study involves complicated phenomena and non-standard approach thereby having useful implications to the scientific and engineering practice.

REFERENCES

1. Japanese Geotechnical Society (1996). *Soils and Foundations, Special Issue on the Geotechnical Aspects of the January 1995 Hyogoken-nambu Earthquake*

2. Tang, T. H., J. Stepp, Y. Cheng, Y. Yeh, K. Nishi, T. Iwatate, T. Kokusho, H. Morishita, Y. Shirasaka, F. Gantenbein, J. Touret, P. Sollogoub, H. Graves and J. Costello (1991). "The Hualien Large-Scale Seismic Test for soil-structure interaction research", *Transactions of the*

Eleventh International Conference on Structural Mechanics in Reactor Technology, Vol. K, pp. 69-74, Tokyo, Japan.

3. Ganev, T., F. Yamazaki and T. Katayama (1995). "Observation and numerical analysis of soil-structure interaction of a reinforced concrete tower", *Earthquake Engineering and Structural Dynamics*, **24**, pp. 491-503.

4. Ganev, T., F. Yamazaki, T. Katayama and T. Ueshima (1997). "Soil-Structure Interaction Analysis of the Hualien Containment Model", *Soil Dynamics and Earthquake Engineering*.

5. Lysmer, J., F. Ostadan, M. Tabatabaie, S. Vahdani and F. Tajirian (1988). SASSI, "A System for Analysis of Soil-Structure Interaction", *User's Manual*, The University of California at Berkeley, CA.

6. Yamada, Y., N. Shiraishi, K. Toki, M. Matsumoto, K. Matsuhashi, M. Kitazawa and H. Ishizaki (1991). "Earthquake-resistant and wind-resistant design of the Higashi-Kobe Bridge", pp. 397-416 in: *Cable-Stayed Bridges, Recent Developments and their Future* (Editors: M. Ito et al.), Elsevier Science Publishers B.V.

7. Japan Road Association (1990). *Specifications for Highway Bridges*.

8. Wolf, J. P. (1985). *Dynamic Soil-Structure Interaction*, Prentice Hall, Englewood Cliffs.

9. The MacNeal-Schwendler Corporation (1995). *MSC/NASTRAN for Windows: Installation and application manual*, Los Angeles, USA.

10. Harada, T., K. Kubo and T. Katayama (1981). "Dynamic soil-structure interaction analysis by Continuum Formulation Method", *Report of the Institute of Industrial Science 29*, University of Tokyo, Japan.

11. Ishihara, K. and I. Towhata (1980). "One-dimensional soil response analysis during earthquakes based on effective stress method", *Journal of the Faculty of Engineering*, The University of Tokyo (B), **35**, (4), pp. 655-700.

12. Katayama, T., F. Yamazaki, S. Nagata, L. Lu and T. Turker (1990). "A strong motion database for the Chiba seismometer array and its engineering analysis", *Earthquake Engineering and Structural Dynamics* **19**, pp. 1089-1106.

13. Towhata, I. and K. Ishihara (1985). "Shear work and pore water pressure in undrained shear", *Soils and Foundations*, JSSMFE, **25**, (3), pp. 73-84.

14. Yamazaki, F., I. Towhata and K. Ishihara (1985). "Numerical model for liquefaction problem under multi-directional shearing on a horizontal plane", *Proceedings of the Fifth International Conference on Numerical Methods in Geomechanics*, Nagoya, Japan.